Small understorey trees have greater capacity than canopy trees to adjust hydraulic traits following prolonged drought in a tropical forest

Running Head: Tropical tree size controls hydraulic responses

Giles, A. L.[1*], Rowland L.[2], Bittencourt P. R. L.[2], Bartholomew, D. C[2], Coughlin I.[4,5], Costa P. B.[1,7], Domingues T.[4], Miatto, R.C[4], Barros, F. V[2], Ferreira L. V.[6], Groenendijk, P[1], Oliveira A. A. R.[6], da Costa A. C. L.[6,7], Meir P.[5,9], Mencuccini M.[10,11], Oliveira R. S.[1]

*Corresponding Author: andregiles.bio@gmail.com, [1]Instituto de Biologia, University of Campinas (UNICAMP), Campinas, SP 13083-970, Brasil.

[1]Instituto de Biologia, University of Campinas (UNICAMP), Campinas, SP 13083-970, Brasil.

[2]College of Life and Environmental Sciences, University of Exeter, Exeter, EX4 4RJ, UK

[3]Biological Sciences, UWA, Perth, WA, Crawley 6009, Australia

[4]Departamento de Biologia, FFCLRP, Universidade de São Paulo, Ribeirão Preto, SP 14040-900, Brasil

[5]Research School of Biology, Australian National University, Canberra, ACT 2601 Australia

[6]Museu Paraense Emílio Goeldi, Belém, PA 66040-170, Brasil

[7] Biological Sciences, UWA, Perth, WA, Australia

[8]Instituto de Geosciências, Universidade Federal do Pará, Belém, PA 66075-110, Brasil

[9]School of GeoSciences, University of Edinburgh, Edinburgh, EH9 3FF, UK

[10]CREAF, Campus UAB, Cerdanyola del Vallés, 08193 Spain

[11]ICREA, Barcelona, 08010, Spain

Abstract

The future of tropical forests is dependent on the capacity of young trees to adjust to drought. We evaluated multiple hydraulic traits indicative of the drought tolerance of small trees across nine common genera at the world's longest-running tropical throughfall exclusion experiment and compared their responses with surviving large canopy trees. Small understorey trees increased specific hydraulic conductivity by 56.3% and leaf:sapwood area ratio by 45.6% in response to the drought treatment. However, understorey trees in both a control and the throughfall exclusion treatment had significantly lower minimum stomatal conductance and maximum hydraulic leaf-specific conductivity relative to the large trees, as well as significantly greater hydraulic safety margin (HSM) and PLC and embolism resitance, occupying a distinctly different hydrualic niche. The greater HSM of small understorey trees relative to large canopy trees likely enables them to adjust other aspects of their hydraulic systems to take advantage of increases in light availability in the understorey, driven by drought-induced mortality of canopy trees. Our results suggest that small understorey trees can adjust their hydraulic systems in response to changes in water and light availability and this has major implications for the regeneration potential of tropical forests following droughts.

Key-words: Long-term drought; Canopy trees; Safety margin; P50; Maximum conductivity; acclimation; Amazon tropical forest.

Introduction

Tropical forests contribute to control the global water and carbon cycles (Houghton 2005; Fan *et al*. 2019). They are responsible for one-third of the net primary production (Corlett 2016), a vital store of carbon (Pan *et al*. 2011) and play a central role in the global water cycle, returning more than 50% of water to the atmosphere (Lovejoy & Nobre 2019). However, the stability and maintenance of carbon stocks and hydrological functioning are threatened by

climate change (Corlett 2016; Brinck *et al.* 2017; Yang *et al.* 2018). Future climate change predictions for tropical forests highlight increased frequency and intensity of extreme drought events (Aragão et al., 2018; Brodribb, Powers, Cochard, & Choat, 2020; Marengo et al., 2018) and long-term reductions in soil moisture availability (Corlett 2016; Christensen *et al.* 2017), which may lead to declines in the carbon sink from elevated tree mortality (Brienen et al., 2015; Green et al., 2019; Hubau et al., 2020; Meir et al., 2015). Most studies relating to drought focus on the impacts on large trees that often comprise the highest proportion of forest biomass (Doughty et al., 2015; Rowland et al., 2015; Yuan et al., 2019). However, understorey trees can be responsible for up to 20% of the forest carbon sink (Hubau *et al.* 2019) and may be critical in determining long-term drought responses if there is extensive loss of the large canopy trees (Bennett et al., 2015; Meir et al., 2015; Rowland, da Costa, et al., 2015).

The effects of drought stress on a plant's hydraulic system has been widely shown to be a key driver of tree mortality (Bittencourt et al., 2020; Brodribb et al., 2020; Rowland et al., 2015). Hydraulic failure occurs when air bubbles (emboli) form in the xylem vessels and as a consequence, there is a severe decrease in the water supply to the leaves. Shortage of water can either directly cause mortality or force plants to close their stomata, reducing photosynthesis and restricting physiological functions (Martinez-Vilalta et al., 2019; McDowell et al., 2008; Sperry et al., 2002). The water potentials at which plant tissues (i.e., stem xylem) lose 50% or 88% of their conductance (P_{50} or P_{88}, respectively) are common measures of xylem embolism resistance (Sperry et al., 2002; Sperry & Tyree, 1988). The difference between the minimum leaf water potential (Ψ_{md}) and P_{50}, known as the hydraulic safety margin (HSM) (Meinzer, Johnson, Lachenbruch, McCulloh & Woodruff 2009), is also critical to a tree's capacity to survive drought (Meinzer *et al.* 2009; Choat *et al.* 2012; Anderegg *et al.* 2016;

Barros *et al.* 2019). Existing studies show limited capacity for tropical trees to adjust their embolism resistance (P_{50}) in response to drought stress (Binks et al., 2016; Bittencourt et al., 2020; Powell et al., 2017; Schuldt et al., 2011), which emphasises the potential role of stomatal control of leaf water potential in order to limit hydraulic damage. Patterns of stomatal closure are likely to be related to a broad set of physiological plant controls, including leaf water potential tolerances (Li et al., 2018; Martin-StPaul, Delzon, & Cochard, 2017; Oren & Pataki, 2001), optimised against the instantaneous demand for carbon by the plant (Eller et al., 2018; Love & Sperry, 2018). Thus, the plant's capacity to tolerate drought is likely to be determined by the interplay of various morphological traits and physiological adjustments associated with the probability of reaching these critical thresholds in response to changes in long term water availability (Choat *et al.* 2018). For example, to maintain a positive carbon balance during prolonged or repeated drought events, it is likely trees will have to adjust their hydraulic system to function beyond the hydraulic safety margins which currently limit their physiology (Christoffersen et al., 2016; Eller et al., 2018).

Leaf physiology and plant architecture have been shown to respond plastically (variations in phenotype in response to environmental change) to drought (Egea *et al.* 2012; Dayer *et al.* 2017; Prendin, Mayr, Beikircher, von Arx & Petit 2018; Yue *et al.* 2019). However studies exploring the plasticity of hydraulic traits remain rare. The few studies of tropical forest drought responses show limited acclimation or plasticity in plant hydraulic traits, including wood anatomy, morphological and physiological traits, in response to drought (Schuldt *et al.* 2011; Powell *et al.* 2017; Tng *et al.* 2018; Bittencourt *et al.* 2020). Other studies have shown that the risk of embolism can be reduced by increasing HSM under drought conditions (Beikircher & Mayr 2009; Awad, Barigah, Badel, Cochard & Herbette 2010; Tomasella *et al.* 2018; Prendin *et al.* 2018). In the only prolonged (>10 year) tropical forest drought

experiment, large trees were found to have limited plasticity in leaf level anatomy (Binks et al., 2016) and no capacity to acclimate their hydraulic systems, especially traits relating to embolism resistance (Bittencourt et al., 2020; Powell et al., 2017; Rowland et al., 2015). However, to our knowledge no studies have evaluated whether small understorey trees (<10 cm diameter at breast height, DBH), have the capacity to adjust their hydraulic system to long-term drought.

When measuring plasticity within plant traits in response to drought, it is important to consider that a range of other important environmental conditions can change together with water availability (Meir *et al.* 2015a). Mortality of large trees can, for example, increase canopy openings and consequently, understorey light availability. This has been shown to increase photosynthetic capacity in small trees (Bartholomew et al., 2020; Metcalfe et al., 2010) and elevates growth rates in lower canopy trees, even following drought (Brando et al., 2008; Rowland et al., 2015). These adjustments most likely resulted in increased stomatal conductance and therefore elevated hydraulic stress within the plant. Consequently, the capacity of a tree to adjust to drought stress is likely to be influenced by whether changes in other resources drive positive or negative feedback on the demand for water and hydraulic stress experienced by the plant.

Most existing research focuses on large trees (defined here as trees with diameter at breast height, DBH, >20 cm). Large trees are likely to be much less limited by changes in light availability that may result from drought-induced mortality in forest stands. Furthermore, their capacity to adjust key hydraulic traits might be lower relative to small understorey trees, because large trees are likely to require many more years to regrow xylem lost to embolism, due to the large total volume of cambium and phloem they maintain, at a substantially higher carbon cost (Trugman *et al.* 2018). Also, as trees develop, their ability to explore different trait combinations is likely to decline because of existing structural and architectural constraints

(Damián, Fornoni, Domínguez & Boege 2018). Consequently, it is likely that small trees can exhibit higher plasticity in their hydraulic systems than large trees, potentially opening up the potential for them to occupy a distinctly different hydraulic niche as they grow under drought conditions compared to pre-existing large canopy trees (Brum *et al.* 2019).

Here we take advantage of a unique drought experiment site in north east Amazonia to evaluate the response of small understorey trees to combined changes in water and light availability. At our experimental site, large trees (>40 cm DBH) had significantly higher mortality rates, when compared to small trees and trees on an equivalent control forest, leading to a 40% reduction in biomass as a consequence of drought (da Costa et al., 2010; Rowland et al., 2015). This biomass loss, almost entirely from the upper canopy, led to an increase in light levels to the understorey, which has driven a significant increase in the annual growth rates of smaller understorey trees, via substantial increases in wet season growth rates (da Costa et al., 2014; Metcalfe, et al., 2010; Rowland et al., 2015). Furthermore elevated radiation loads are likely to have increased leaf vapour pressure deficit and temperature, increasing the atmospheric drought effect these understorey trees experience (Mulkey & Pearcy 1992a; Kamaluddin & Grace 1992; Krause, Virgo & Winter 1995). Therefore even without changes in soil moisture availability, taking advantage of the increased light availability to grow, should require plants to change their hydraulic system to increase water supply and/or sustain lower xylem water potential driven by the increasing atmospheric water demand. Using new data from this unique drought experiment site, we explore how understorey trees adjust to increases in light availability coupled with increased drought stress, determining if drought stress prevents trees from adjusting to elevated light conditions. We test how understorey trees (1-10 cm DBH), henceforth small understorey trees, alter their plant hydraulic system in response to prolonged soil moisture stress and increased canopy openness, and determine how these responses vary relative to those of large trees (>20 cm DBH). We address the following key hypotheses:

1) The hydraulic system of small trees adjusts to the combined soil drought and radiation load conditions imposed in the TFE relative to the Control. We expect the small understorey trees in TFE treatment to have more negative water potential values and higher hydraulic safety margins to increase water transport efficiency to meet elevated canopy water demands.

2) Small understorey trees have a different hydraulic strategy to large canopy trees. Overall, we predict that, relative to large trees, small trees will have different hydraulic traits (size effect). Specifically, we predict that traits characteristic of stress tolerance (whether caused by low radiation in the Control or low water availability in the TFE), i.e., more negative predawn and midday water potentials, higher xylem embolism resistance, larger hydraulic safety margin and lower minimum stomatal conductance would occur in small trees. We also predict that small trees will be more responsive to the changes in the TFE plot (tree size-plot interaction) partly as a consequence of the fact that small trees experienced larger changes in radiation load across the two plots. Hence, we expect these hydraulic traits to change more in small trees in the TFE even in the face of the risk of higher dry season losses of conductivity.

3) Trait adjustments during development from understorey to canopy trees and in response to the TFE treatment are significantly influenced by taxonomic identity. We expect the comparisons among small trees, and between small and large trees are influenced by a taxonomic effect that reflects the evolutive history and consequently causes variation in the drought response.

Methods

Site and plant material

Our study site is a lowland tropical rainforest located in the Caxiuanã National Forest, state of Pará, north-east Brazil (1°43′S, 51°27 W). It has an annual rainfall of 2000-2500mm, with a dry season (< 120 mm monthly rainfall) from July to December. A throughfall exclusion

(TFE) experiment was established in 2002, where 50% of canopy throughfall is excluded by a plastic panel structure installed at 1-2m height over a 1 ha area. The TFE plot was studied alongside a 1 ha control plot, where no throughfall removal took place. The plots have been monitored continuously since 2001 and further information on the experimental set-up can be found in earlier papers (da Costa *et al.*, 2010; Fisher *et al.*, 2007; Meir *et al.*, 2015 and Rowland *et al.*, 2015b).

From August-September 2017, during peak dry season, we sampled 74 small understorey trees with diameters ranging from 1 to 10 cm at breast height (1.3 m). Forty-one small understorey trees were measured on the control plot and 33 on the TFE, all taken from nine genera (20 species total), replicated in each plot (two to five individuals per plot). It was not possible to know the age of each sampled individual, because destructive sampling for age determination (tree-ring analyses, Brienen et al., 2016) was not possible. Consequently, we must assume that our sample trees could have strongly varying ages (Groenendijk, Sass-Klaassen, Bongers & Zuidema 2014). Therefore here we considered our hypotheses regarding these understorey trees to be mostly related to tree stature and position within the forest strata, acknowledging that it is most likely that a majority, but not all of, our sample trees are likely to be young juveniles (Van Der Sleen et al 2015).

For each individual, we collected two branches from the top of the crown, representing the point maximally exposed to light. The branches were third to fourth order, counting from the leaves. We collected one set of branches before sunrise (0400 to 0600 hours) and used these to measure embolism resistance and predawn leaf water potential. We collected a second set of branches at midday (1130 to 1330 hours) and used these to measure midday leaf water potential, native embolism, leaf-to-sapwood area, xylem and leaf specific conductivity, minimum leaf conductance and wood density measurements. Immediately after collection, branches were bagged in thick black plastic sacks with moist paper to humidify

internal air and minimise leaf transpiration. Branches were transported 100 m from the plots to measure leaf water potential, and for the remaining measurements the branches were transported to a laboratory 30 minutes away. In all branches, heartwood was absent and pith area was either absent or negligible.

We measured predawn water potential (Ψpd). This measure is taken when transpiration is at its minimum and the water potential of the plant is closest to equilibrium with that of the soil. Ψpd can be considered an integrated metric of maximum soil water availability across the rooting depth (Bartlett et al. 2016). we also determined midday water potential (Ψmd), to capture the minimum Ψ of the plant in the dry season. This measure is affected by any cuticular or stomatal transpiration and, thus, broadly captures the integrated effects of plant traits and the environment on the minimum water potential a plant reaches in natural conditions. All water potential measures are expressed in negative values. We also measured the native dry season percentage loss of conductivity (PLC) and we used the difference between the minimum leaf water potential (Ψ_{md}) and P_{50}, to calculate the hydraulic safety margin (HSM). These two values (native PLC and HSM) were used as indicators of the cumulative damage from embolism.

Predawn and midday water potential

Predawn and midday leaf water potentials (Ψpd) were measured in the field immediately after collection, using a pressure chamber (Model 1505, PMS), without being bagged. Branches collected for predawn water potential measures were sampled before sunrise, between 0400 to 0600 hours, and for midday water potential, the sampling took place between 1130 to 1330 hours. For each tree we measured water potential of two leaves, or three leaves if the first two measures differed substantially (>0.5 MPa difference) from one another. Measurements from multiple leaves were averaged to create a single value per tree.

Wood density, leaf to sapwood area *ratio and minimum stomatal conductance*

We measured wood density on woody sections 40 to 80 mm long and 4 to 7 mm diameter cut from the branch. We debarked samples, immersed them in water for 24 hours to rehydrate and measured saturated volume using the water displacement method (Pérez-Harguindeguy *et al.*, 2013). We then oven dried the samples at 60°C for 48 hours and measured their dry weight with a precision balance.

We determined the leaf to sapwood area ratio (A_L:A_{SW}), on all branches by measuring leaf area and calculating sapwood area from two diameter measurements of the debarked basal part of the branch using precision callipers. We measured leaf area by scanning all leaves on the branch and quantifying their area using Image J software (version 1.6.0_20; Schneider et al., 2012). We calculated the leaf area to sapwood area ratio as total branch leaf area divided by basal sapwood area.

For minimum leaf conductance (G_{min}), we used the leaf conductance to water vapour measured in the abaxial surface of leaves kept 30 minutes in the dark, using an infrared gas analyser (Li-COR 6400, US). All leaves measured were fully-formed, undamaged leaves. G_{min} is likely a combination of stomatal conductance from leakage of partially closed stomata and cuticular conductance (see Rowland *et al.* 2020) and Bartholomew et al., (2020), for further leaf gas exchange measurement details).

Hydraulic efficiency and native embolism

We calculated maximum hydraulic specific conductivity (K_s) as a measure of xylem hydraulic efficiency and maximum leaf specific conductivity (K_{sl}) as a measure of leaf water supply capacity. We used the native percentage loss of conductivity of the collected branches (PLC) as a measure of native embolism. To estimate these variables, we measured branch xylem hydraulic conductivity before (K_{snat} – native conductivity) and after flushing to remove emboli and we quantified the leaf area distal to the sample to obtain K_{sl} from K_l (leaf

conductance). Using samples from the branches collected at midday, we put the entire branch underwater and discarded a 10 cm long segment from the base. After this, we cut another 10-15 cm long segments from each branch base underwater and let them rehydrate for 15 min to release tension and avoid artefacts (Venturas, Mackinnon, Jacobsen & Pratt 2015). Subsequently, to relax the tension in the branch we cut 1-1.5 m of branch from base to leaves underwater, in steps of ~15 cm, and used the distal end of the branch for hydraulic measurements, to ensure no artificially embolised vessels were present in the measured sample. All samples used for hydraulic measurements were second or third order branches, between 30-55 mm in length and 3-5 mm diameter and were recut underwater with a sharp razor blade before connecting to the apparatus, to ensure all vessels were open at both ends. We then measured flow using the pressure drop over a capillary method (Pereira & Mazzafera 2013), where a capillary of known conductance is connected in series with the sample to measure K_s and then the samples are flushed to remove emboli and estimate maximum conductance (Martin-StPaul et al., 2014). We note the samples remain under-water at all times for this entire procedure. We calculated PLC as the ratio of K_{snat} to K_s multiplied by 100. We calculated K_{ls} as the sample hydraulic conductivity (i.e. sample conductance times sample length) after flushing divided by the leaf area distal to the measured sample.

Embolism resistance and hydraulic safety

As an index of xylem embolism resistance, we used P_{50} and P_{88}, the xylem water potentials where, respectively, 50% and 88% of hydraulic conductivity is lost. We also used P_{50} to calculate the hydraulic safety margin - the difference between P_{50} and Ψ_{md}, an index of tree hydraulic safety. Branches collected before sunrise were rehydrated for 24 hours and from each branch we cut two or three smaller branches of approximately 40-70 cm. We measured the xylem embolism resistance of each branch using the pneumatic method (Pereira *et al.* 2016; Zhang *et al.* 2018). With this method, the loss of hydraulic conductance is estimated

from the increase in air volume inside the wood caused by embolism formation as the branch dehydrates. Air volume is estimated from the air discharge from the cut end of the branch into a vacuum reservoir (~50 kPa absolute pressure) of known volume during a given amount of time (2.5 minutes). We measured initial and final pressure inside the vacuum reservoir with a pressure transducer (163PC01D75, Honeywell) and calculated the volume of air discharged using the ideal gas law. A detailed protocol is presented in (Bittencourt, Pereira & Oliveira 2018). Percentage loss of conductance for each branch is estimated from percentage air discharged (PAD) during the course of its dehydration. PAD is calculated by standardizing air discharge for each branch by its minimum (fully hydrated) and maximum (most dehydrated) air discharge state. We dehydrated branches using the bench dehydration method. Before each air discharge measurement, branches were sealed in thick black plastic bags for one hour for leaf and wood xylem water potential to equilibrate. Directly after the air discharge was measured, we estimated wood xylem water potential by measuring the leaf water potential of one to two leaves. Drought embolism resistance is then given by the increase in PAD with decreasing xylem water potential for each tree. To calculate P_{50}, we pooled data from the two-three branch replicates from the same tree and fitted a sigmoid curve to the data, where P_{50} and slope (a) are the fitted parameters (Pammenter & Van der Willigen 1998) and P88 is predicted from the fit (Eqn 1):

$$\mathrm{PAD} = 100/\left(1 + \exp\left(a\left(\Psi - \mathrm{P50}\right)\right)\right)$$

Eqn1. Percentage air discharge equation (PAD). Ψ Water potential. P_{50} (-xylem embolism resistance (MPa)

Data analysis

By comparing trees found on the control and TFE experimental plots, we measure the effect of the experimental drought on our drought stress indicators (Ψ_{pd} - predawn water potential;

Ψ_{md} - midday water potential; HSM – hydraulic safety margin to P_{50}; PLC – native dry season percentage loss of conductivity) and plant traits (W_D – wood density; A_L:A_{SW} - leaf to sapwood area; P_{50} - xylem embolism resistance; P_{88} - xylem embolism resistance; G_{min} – minimum stomatal conductance; K_s – maximum hydraulic specific conductivity; K_{sl} - maximum hydraulic leaf -specific conductivity) in small understorey trees. We used linear mixed effects models in the package lme4 (Bates, Mächler, Bolker & Walker 2015) to test for plot (TFE vs control) and taxonomic effects (genus and species) on hydraulics traits in small trees (n = 66). We started with a full fixed and random effect model of the plot, genus and their interaction. We Tested the significance of the random effect by removing it and evaluating if the model significantly worsened. We tested sequentially for the random effect of genus on: (a) the model intercept; (b) the model plot without intercept; and (c) both intercept and plot. When more than one random effect format was significant, we chose the most parsimonious random effect (i.e. intercept effect only), unless the Akaike information criterion (AIC) of the more complex model was at least 2 units lower than the simpler model. After testing the random effects, we tested the fixed effects by first removing the interaction (plot with genus) and testing if this significantly worsened the model and after this using the same approach with the additive terms. If no random effect was significant (lmerTest), we changed to a fixed effect model (R base package 'lm' function) and analysed fixed effects in the same way. When the taxonomy was included (genus and specie) as a random effect in our models, we tested for genus and species nested within the genus taxonomic effect. we tested the complete model (genus and species as a random effect) against a GLM only fixed effects, then if significant we keep the random effect. When genus was not significant, linear models were used to test the significance of the fixed effects. To quantify model goodness of fit, we considered the marginal and conditional R^2 (Mulkey & Pearcy 1992b). The marginal R^2 indicates how much of the model variance is explained by the fixed effects only, whereas the conditional R^2 indicates

how much of the model variance is explained by the complete model, fixed and random effects. All the analyses were done in R (version 3.3.0; R Core Team, 2016)

Small and large tree comparisons

We tested for differences in individual tree-level responses to the TFE treatment for large (n = 72) and small trees (n = 39). We use the large trees data from Bittencourt et al. (2020) conducted in the same experimental plots and collected during the same period with the same methodological procedures. For this comparison we restrict the samples to those trees whose genera are replicated on both plots and between the large and small trees, with a minimum sample size of 2 individuals per size group per plot and genus. Consequently, the number of genera and individuals employed in this comparison is lower than the available number of individual small understorey trees and the full data-set published within Bittencourt et al., (2020). In total we use five genera (*Eschweilera*, *Inga*, *Licania*, *Protium*, *Swartzia*), with 15 small understorey tree on the Control and 24 small understorey trees on the TFE, and 35 large trees on the Control and 37 large trees on the TFE. We used linear mixed effect models to test the effects of the TFE treatment, tree size with two classes (Large and Small), and the interactions between treatment and tree size on drought stress indicators and hydraulic traits. Taxonomic effects were included by using genus as random effects, following the same protocol used for small tree analyses. We selected the best model from a full model set according to the Akaike information criterion with a correction for small sample sizes (AICc scores) (Barton, 2018). Within this paper, all data presented represent the mean and associated errors denote standard errors of the mean. A summary of available trait data by genus is presented in Table 1.

Results

The reduced soil moisture availability and increased canopy openness caused by 15 years of the Throughfall Exclusion Experiment (TFE) (Figure S1) caused significant changes in the

hydraulic traits of the small understorey trees (Figure 1). Maximum specific conductivity (K_s) increased by 56.3±41.5% in the TFE small trees relative to the control (Figure 1, $p<0.01$), similarly there was a 45.6±38.2% increase in the leaf: sapwood area ratio (Figure 1; $p<0.001$). The TFE also had significant effects on drought stress indicators (Figure 1), including predawn and midday water potential (Ψ_{pd}, Ψ_{md}). Ψ_{pd} was 0.56 MPa lower on the TFE relative to the control ($p <0.001$) and Ψ_{md} 0.61 MPa ($p < 0.001$) lower. In contrast other key hydraulic traits including xylem embolism resistance (P_{50} and P_{88}), leaf specific conductivity (K_{sl}), minimum stomatal conductance (G_{min}) and wood density (W_D) showed no significant change between the TFE and the Control plots (Figure1; Table 2; Table S1).

Genus effects on hydraulic traits and their interactions with drought

Using mixed-effect modelling analysis we found that variance explained by taxonomy had only a limited role in affecting the overall drought responses. Of the four variables which demonstrated significant changes in trait values in response to the TFE, only for Ψ_{md} did genus or species nested within genus significantly influence the intercept of the relationship with drought treatment (Table 2). When genus by genus responses to the drought effect were examined separately, it was clear that there were highly variable responses to the treatment within genera, however these were inconsistent in terms of direction and magnitude. We cannot separate the taxonomic effect from the residual variance because genus-specific influences on the plot effect were highly variable (Figure 2). Given the low replication (between 2 and 5 for each genus on each plot treatment) and high variation within each genus, it was not always statistically viable to test the plot effect within each genus (Figure 2), however where this was possible, clear statistical differences were seen for some genera (Kruskal-Wallis test) but not for others. For example, *Inga* showed consistent response in leaf:sapwood ratio and K_s while *Ocotea* did not show differences between plots (Figure 2). K_s

showed the most consistent drought treatment response across all genera, as, with the exception of *Ocotea* and *Tetraglatris*, all other genera showed a clear, significant, increase in K_s on the TFE (Figure 2). The patterns described here were also maintained when we analysed the data at a species level (data not shown).

Large versus small trees

We compared the responses of hydraulic traits between large trees (>20 cm DBH) and small understorey trees (1-10 cm DBH). With the exception of Ψ_{pd}, the results we obtain considering only the five genera, which were also sampled within the canopy tree study, were similar to when considering all nine genera of understorey trees present in control plot and TFE experiment (see Figure S3 supplementary , Table S2 for models significance and Table S3 for n values for the small to large tree comparisons).

In contrast to the large increase in K_s observed in the small trees (Figure 1 & S3), the plot level average values of K_s are similar among large trees (4.82±3.93 TFE and 4.86±2.79 Control plot). Similarly for Ψmd, where large plot level differences were found in small trees, showed limited plot level differences among large trees (-1.72 ± 0.48 TFE and -1.70±0.48 Control treatment). However, small understorey trees have values of Ψ_{md}, which are 17.12±0.03% higher (values closer to 0) than for than canopy trees. Furthermore, for the variables which had no treatment effect amongst the small trees we find on average, across both the TFE and Control plots, the small understorey trees have a 38.2±32.1% ($p<0.01$) more negative P_{50} and a 68.4±58.8% and 20.7±30.4% lower G_{min} and K_{sl}, respectively, relative to the large trees (Figure, 3b, 3d, 3f; $p<0.001$). HSM and PLC were 72.97±36.34% and 44.41±14.62% greater, respectively, in the small understorey trees relative to large trees (Figure, 3g, 3i, 3j; $p<0.01$).

We analysed the influence of genus on the combined effect of treatment and tree size effect (i.e. large and small trees on the control and TFE plot) for the five genera we could replicate across plots and tree size classes. We found that the effects of tree size varied substantially among genera (Figure 4). For example, the difference in P_{50} between adult trees and the small understorey trees was 61.48±52.51% for Licania and 38.96±3.7% for *Inga* (Figure 4). In contrast, Gmin was consistently significantly lower in the small understorey trees relative to large trees across almost all genera (Figure 4b). It is also clear that the patterns of response to

410 the drought changes when we see only to genus and compare the large and small trees within
411 certain taxa, for example, Inga mean P_{50} has a significant difference between control and TFE
412 for both small and large trees (Figure 4). A difference in traits values between the Control and
413 TFE plots that was present either for small tree or large trees but not both size classes
414 simultaneously, occurred multiple times (Figure 4), especially for the genus *Inga*. We note
415 the relatively low replication per genus, per plot, per size group (n values from 2-8 individuals)
416 and high intra-genus variation (Figure 4), makes the interpretation of genus level differences in
417 traits complex. Mixed effect modelling results did however, identify a strong influence of genus
418 on trait variation between our two size classes (Table 2), yet there are limited cases where we
419 find significant models demonstrating trait differences between the Control and the TFE plot
420 have a significant tree size and genus effect (Table 2).

421

422 **Discussion**

423 We find that small understorey trees (1-10 cm DBH) have the capacity to increase maximum
424 specific hydraulic conductivity and leaf to sapwood area ratio in response to prolonged (15
425 year) soil moisture stress. Despite having significantly lower pre-dawn and midday leaf water
426 potentials, alongside soils with significantly lower soil moisture contents, small trees have the
427 capacity to adjust key hydraulic traits to permit a positive response to a higher light
428 environment.This suggests that despite the soil drought stress, small understorey trees can still
429 increase water transport efficiency and crown water demand in response to increases in light
430 availability, following the drought-induced mortality of large top canopy trees, potentially
431 allowing them to maximise the productivity in periods of the year when water is available. We
432 also show that small understorey trees have a very distinct hydraulic reponse relative to large
433 trees on the canopy. Although they had many more embolized vessels (higher PLC in smaller

understorey trees relative to canopy tree on the TFE), these smaller trees were still able to acclimate more hydraulic traits to a much greater degree than large canopy trees.

Following the first eight years of the experimental drought, a substantial increase in the mortality rate of largest trees was observed, leading to a substantial loss in biomass from canopy trees (da Costa et al., 2010; Rowland et al., 2015). This partial loss of the upper canopy led to an increase in the light availability in the lower canopy of the TFE, driving increases in the maximum photosynthetic capacity (71.1% and 29.2% increase in Jmax and Vcmax respectively) and a 15.1% increase in the LMA of the same understorey small trees we study here (Bartholomew *et al.* 2020). These types of differences in response to the prevailing light environment have also been observed elsewhere in tropical tree canopies (Ruggiero, Batalha, Pivello & Meirelles 2002; Domingues *et al.* 2010; Cavaleri, Oberbauer, Clark, Clark & Ryan 2010) and are indicative of plants changing their allocation strategy in response to increased light availability (Poorter et al., 2009; Wright et al., 2004). Critically, these allocation shifts are likely to result in a net increase in photosynthesis and growth (Metcalfe et al., 2010; Rowland et al., 2015), which require higher water supply to the canopy of each individual. The elevated soil moisture stress in the TFE relative to the control trees, manifested itself as significantly more negative pre-dawn and midday leaf water potential values (Figure 1h e 1i), key indicators of plant water stress (Bhaskar & Ackerly, 2006; Kramer, 1988; Martínez-vilalta & Garcia-Forner, 2017). Interestingly, these more negative water potentials did not translate into a significant change in HSM between plots, due to a trend, albeit statistically insignificant, towards more negative P_{50} values on the TFE plot trees relative to those on the Control (Figure 1). When examined at the genus level, five of the nine genera have consistently more negative P_{50} values on the TFE relative to the Control, with two remaining roughly equal and two less negative on the TFE (Figure 2). These data suggest that, despite operating at more negative water potentials, it is still possible for small understorey trees to adjust their hydraulic system to support the increased growth in response to greater light availability.

460 Consistent with increases in photosynthetic capacity, we observe an increase in leaf
461 area to sapwood area ratio in the small understorey trees on the TFE, relative to the Control.
462 This demonstrates that these trees are increasing the total photosynthesising leaf area per unit
463 of stem area. A global study, including multiple sites from the tropics has shown that a plant's
464 hydraulic system is highly sensitive to changes in this ratio, which may be one of the main
465 factors controlling trade-offs in other plant hydraulic traits (Mencuccini *et al.* 2019). The
466 increase in leaf area would increase the total water demand of the tree. However, the
467 observed increases in photosynthetic capacity (High values of Vcmax and Jmax Bartholomew
468 et al. 2020), may allow slightly lower stomatal conductance for any given CO_2 concentration
469 (Bartholomew et al., 2020; Sperry et al., 2017). This may, in part, compensate for the increase
470 in demand for water which elevated leaf areas may cause. However, even with the observed
471 increases in photosynthetic capacity, these small understorey trees probably still experience
472 increased total water demand, suggesting that small trees must increase maximum hydraulic
473 conductivity and/or tolerate reductions in water potential and therefore greater embolism risk
474 (Sperry et al., 2017). Our data show that the small understorey trees on the TFE plot respond
475 to this increased canopy water demand by increasing K_s (Figure 1f) relative to the to their
476 counterpart small trees in the Control, but they do not show significant changes in embolism
477 resistance (P_{50}, P_{88}), despite the observed trend towards lower values on the TFE (Figure 1k).
478 The lower plasticity of P_{50} to drought is consistent with other data from this study site
479 (Bittencourt et al 2020; Rowland et al 2015; Powell et al 2018), suggesting a low capacity to
480 adjust vulnerability to xylem embolism (Maherali, Pockman & Jackson 2004). However, these
481 studies also found limited plasticity in K_s in response to drought, further supporting the idea
482 that our observed changes in traits are more likely to be driven by changes in canopy light
483 availability than drought and made possible by ontogenetic stage.

484 Our data suggest that to tolerate the prolonged reduction in both pre-dawn and midday leaf
485 water potential, small understorey trees must have a greater capacity to tolerate drought

stress and/or a greater potential to re-grow new xylem to replace old xylem (Nardini, Lo Gullo & Salleo 2011a; Brodersen & McElrone 2013). Our comparison between small understorey trees and large canopy trees suggests that smaller trees do indeed have a very different water use strategy. The differences in the traits we observe were far greater, and in most cases significantly so, between the large and the small trees than for trees of the same size between treatments, for either size class. We show that smaller trees across both the Control and the TFE plot have significantly lower P_{50} values and G_{min} values and significantly greater hydraulic safety margins, midday leaf water potentials and PLC (Figure 3). Consistent with the results from large scale studies (e.g. Choat et al., 2012), where taxonomic matching between size classes was not conducted and small trees (<10cm) were not considered, in our study we find the HSM is 1.94MPa more positive in the small understorey trees relative to large trees, where they are close to zero on both plots. If we assume that the smaller trees in this study are shallow-rooted, this outcome is consistent with findings that shallow-rooted species, compensate for the lack of access to deep water through developing greater xylem embolism resistance and strong stomatal control (Brum et al., 2019; Tardieu, 1996, Sperry et al. 2017). This greater hydraulic safety margin, is likely to be what is enabling smaller trees to adjust to increased light availability, despite the lower water availability in this treatment, as it enables these trees to tolerate greater drought stress without passing critical thresholds. Furthermore, the carbon gain associated with allowing greater photosynthesis when higher light is available is more likely to be translated into new xylem growth in smaller understorey trees, meaning rapid replacement of damaged tissues is likely to be more viable in these smaller trees, relative to large top canopy trees (Damián *et al.* 2018; Trugman *et al.* 2018). This likely means that the risk associates with higher PLC levels is reduced. Combined these factors allow small understorey trees to have greater flexibility in terms of the strategy they use to adapt to combined changes in water and light availability.

511 Relative to large trees, smaller trees are likely to be more constrained by light
512 availability and more at risk of limitations in carbon supply (McDowell et al., 2011; McDowell &
513 Sevanto, 2010). The maximum opportunity for shaded understorey trees to generate carbon
514 for growth in tropical forests occurs during the dry season when cloudiness is lower and
515 available incident radiation is higher (Carswell 2002), but conversely these periods are
516 characterised by the largest water deficit in the superficial layers of the soil (Poorter *et al.*
517 2009; Sterck, Anten, Schieving & Zuidema 2016). However, the larger safety margin in small
518 understorey trees is likely to substantially reduce risk of mortality (Eller et al., 2018; Eller et
519 al., 2020; Love & Sperry, 2018; Sperry et al., 2017). Furthermore, maintaining significantly
520 lower G_{min} and higher midday leaf water potential (Figure 3d, g), relative to the large trees,
521 despite having similar pre-dawn leaf water potentials, suggests that these small trees are able
522 to more tightly regulate water loss, during both the day and night. Consequently, this greater
523 degree of control further reduces the risk of runaway embolism when photosynthesising
524 during periods with low Ψ_s, particularly if these trees can repair cavitated vessels (Nardini et
525 al., 2011; Salleo et al., 2004; Salleo et al., 1995, Rowland et al., 2015) or grow new vessels
526 between consecutive dry seasons (Eller *et al.* 2018).

527 The response of small trees to both light and drought can be highly variable and was
528 not independent of taxonomy. For the small understorey trees, two of the four variables we
529 found to significantly change between treatments (K_s and Ψ_{md}) were influenced by genus
530 within our mixed effect modelling analysis. When the responses of these trees to the
531 experiment are plotted separated by genus, it is clear that there are very large variations in the
532 direction and magnitude of the trait changes in response to the drought effect, as well as very
533 larger intra-genus variation (Figure 4 and Figure S2). Furthermore, all of the six variables for
534 which we found a tree size effect within our models (Table 3) had a significant genus effect on
535 the intercept. When examined at a genus by genus level (Figure 4) high levels of intra-genus
536 variation still exist, but for most genera the size-driven differences are very larger and remain

much clearer than the treatment differences (Figure 4). This suggests that despite the stronger effect of taxonomy on the changes in traits, size-dependent changes are larger and stronger than drought and/or light-induced changes in traits. We acknowledge the complexity of interpreting results at the genus level within our analysis, given the limited capacity to generate high replicates within each taxonomic group for this diverse tropical forest and the high within taxon variation we observe. Our results concerning taxonomy are consistent with a growing literature from tropical forests showing the importance of considering the complex role that taxonomy plays in influencing hydraulic responses to environmental change (Barros et al., 2019; Bittencourt et al., 2020; Brum et al., 2019; Oliveira et al., 2019). However, our results offer new insights here, in that we are able to show a consistently larger impact of tree size and canopy position on traits regulating plant water use.

This study highlights the importance of forest structural change in controlling the traits of what are likely to be the next generation of trees growing up during prolonged drought stress. We show that small understorey trees have higher capacity to acclimate their hydraulic systems to increases in understorey light availability following drought-induced mortality of canopy trees relative to large top canopy trees. Small trees are able to acclimate despite experiencing prolonged soil moisture stress, which resulted in lower leaf water potentials and greater PLC. Our results demonstrate that there is a consistent and larger shift in the plant hydraulic strategy of saplings relative to large trees across most of Amazonia's hyper-abundant taxonomic groups. A key uncertainty which remains to be answered, however, relates to the long-term development of these understorey trees. Assuming these small trees continued to develop under the experimental drought stressed conditions, it would be of interest to know if the trajectory of change in hydraulic traits we observe can be sufficient to increase the hydraulic resistance of these trees as they approach full size. Ultimately, continued acclimation of hydraulic systems throughout a tree's lifespan may allow a more drought-resilient ecosystem to develop.

Acknowledgements

Thank the UNICAMP postgraduate program in Ecology the Brazilian Higher Education Co–ordination Agency (CAPES). This work is a product of a UK NERC independent fellowship grant NE/N014022/1 to LR. It was also supported by a UK NERC grant NE/J011002/1 and EU FP7-Amazalert to PM to PM and MM, CNPQ grant 457914/2013-0/MCTI/CNPq/FNDCT/LBA/ESECAFLOR to ACLD, and an ARC grant DP170104091 to PM and FAPESP/Microsoft research (grant 11/52072–0) awarded to RSO. DB is supported by a UK NERC studentship NE/L002434/1. P.R.L.B acknowledges Royal Society's Newton International for its Fellowship (NF170370).

Conflict of interest

The authors have no conflict of interest to declare.

Authorship

ALG collected and compiled the data alongside LR, PRLB, IC, PBC, LVF, DDV, JASJ, DCB and ACLdC. LR designed the study with MM, ACLdC, PM and RO. ALG, PRLB and LR performed the statistical analysis and ALG, LR and RO wrote the paper, all other authors substantially contributed to revisions.

References

Anderegg W.R.L., Klein T., Bartlett M., Sack L., Pellegrini A.F.A. & Choat B. (2016) Meta-analysis reveals that hydraulic traits explain cross-species patterns of drought-induced tree mortality across the globe. *PNAS* **113**, 2–7.

Aragão L.E.O.C., Anderson L.O., Fonseca M.G., Rosan T.M., Vedovato L.B., Wagner F.H., … Saatchi S. (2018) 21st Century drought-related fires counteract the decline of Amazon

587 deforestation carbon emissions. *Nature Communications* **9**, 536.

588 Awad H., Barigah T., Badel E., Cochard H. & Herbette S. (2010) Poplar vulnerability to xylem
589 cavitation acclimates to drier soil conditions. *Physiologia Plantarum* **139**, 280–288.

590 Barros F.D. V, Bittencourt P.R.L., Brum M., Restrepo–Coupe N., Pereira L., Teodoro G.S., …
591 Oliveira R.S. (2019) Hydraulic traits explain differential responses of Amazonian forests to
592 the 2015 El Niño–induced drought. *New Phytologist* **223**, 1253–1266.

593 Bartholomew D.C., Bittencourt P.R.L., Costa A.C.L., Banin L.F., Britto Costa P., Coughlin S.I., …
594 Rowland L. (2020) Small tropical forest trees have a greater capacity to adjust carbon
595 metabolism to long–term drought than large canopy trees. *Plant, Cell & Environment* **43**,
596 2380–2393.

597 Bates D., Mächler M., Bolker B.M. & Walker S.C. (2015) Fitting linear mixed-effects models
598 using lme4. *Journal of Statistical Software* **67**.

599 Beikircher B. & Mayr S. (2009) Intraspecific differences in drought tolerance and acclimation in
600 hydraulics of Ligustrum vulgare and Viburnum lantana. *Tree Physiology* **29**, 765–775.

601 Bennett A.C., Mcdowell N.G., Allen C.D. & Anderson-Teixeira K.J. (2015) Larger trees suffer
602 most during drought in forests worldwide. *Nature Plants* **1**, 1–5.

603 Bhaskar R. & Ackerly D.D. (2006) Ecological relevance of minimum seasonal water potentials.
604 *Physiologia Plantarum* **127**, 353–359.

605 Binks O., Meir P., Rowland L., Costa A.C.L., Vasconcelos S.S., Oliveira A.A.R., … Mencuccini M.
606 (2016) Plasticity in leaf–level water relations of tropical rainforest trees in response to
607 experimental drought. *New Phytologist* **211**, 477–488.

608 Bittencourt P.R.L., Oliveira R.S., Costa A.C.L., Giles A.L., Coughlin I., Costa P.B., … Rowland L.
609 (2020) Amazonia trees have limited capacity to acclimate plant hydraulic properties in

610 response to long−term drought. *Global Change Biology* **26**, 3569–3584.

611 Bittencourt P.R.L., Pereira L. & Oliveira R.S. (2018) Pneumatic Method to Measure Plant Xylem
612 Embolism Paulo. *bio-protocol* **8**, 1–14.

613 Brando P.M., Nepstad D.C., Davidson E.A., Trumbore S.E., Ray D. & Camargo P. (2008) Drought
614 effects on litterfall, wood production and belowground carbon cycling in an Amazon
615 forest: results of a throughfall reduction experiment. *Philosophical Transactions of the*
616 *Royal Society B: Biological Sciences* **363**, 1839–1848.

617 Brienen R., Schongart J. & Zuidema P. (2016) *Tropical Tree Physiology*. (eds G. Goldstein & L.S.
618 Santiago), Springer International Publishing, Cham.

619 Brienen R.J.W., Phillips O.L., Feldpausch T.R., Gloor E., Baker T.R., Lloyd J., … Zagt R.J. (2015)
620 Long-term decline of the Amazon carbon sink. *Nature* **519**, 344–348.

621 Brinck K., Fischer R., Groeneveld J., Lehmann S., Dantas De Paula M., Pütz S., … Huth A. (2017)
622 High resolution analysis of tropical forest fragmentation and its impact on the global
623 carbon cycle. *Nature Communications* **8**, 14855.

624 Brodersen C.R. & McElrone A.J. (2013) Maintenance of xylem network transport capacity: A
625 review of embolism repair in vascular plants. *Frontiers in Plant Science* **4**, 1–11.

626 Brodribb T.J., Powers J., Cochard H. & Choat B. (2020) Hanging by a thread? Forests and
627 drought. *Science* **368**, 261–266.

628 Brum M., Vadeboncoeur M.A., Ivanov V., Saleska S., Alves L.F., Penha D., … Oliveira R.S. (2019)
629 Hydrological niche segregation defines forest structure and drought tolerance strategies
630 in a seasonal Amazon forest. *Journal of Ecology*, 318–333.

631 Carswell F.E. (2002) Seasonality in CO 2 and H 2 O flux at an eastern Amazonian rain forest.
632 *Journal of Geophysical Research* **107**, 8076.

633 Cavaleri M.A., Oberbauer S.F., Clark D.B., Clark D.A. & Ryan M.G. (2010) Height is more
634 important than light in determining leaf morphology in a tropical forest. *Ecology* **91**,
635 1730–1739.

636 Chadwick R., Good P., Martin G. & Rowell D.P. (2016) Large rainfall changes consistently
637 projected over substantial areas of tropical land. *Nature Climate Change* **6**, 177–181.

638 Choat B., Brodribb T.J., Brodersen C.R., Duursma R.A., López R. & Medlyn B.E. (2018) Triggers
639 of tree mortality under drought. *Nature*.

640 Choat B., Jansen S., Brodribb T.J., Cochard H., Delzon S., Bhaskar R., … Zanne A.E. (2012) Global
641 convergence in the vulnerability of forests to drought. *Nature* **491**, 752–755.

642 Christensen J.H., Krishna Kumar K., Aldrian E., An S.I., Cavalcanti, I.F.A. de C., … Zhou T. (2017)
643 Climate Phenomena and their Relevance for Future Regional Climate Change. In *Climate*
644 *Change 2013: The Physical Science Basis. Contribution of Working Group I to the Fifth*
645 *Assessment Report of the Intergovernmental Panel on Climate Change*.

646 Christoffersen B.O., Gloor M., Fauset S., Fyllas N.M., Galbraith D.R., Baker T.R., … Meir P.
647 (2016) Linking hydraulic traits to tropical forest function in a size-structured and trait-
648 driven model (TFS v.1-Hydro). *Geoscientific Model Development* **9**, 4227–4255.

649 Corlett R.T. (2016) The Impacts of Droughts in Tropical Forests. *Trends in Plant Science* **21**,
650 584–593.

651 da Costa A.C.L., Galbraith D., Almeida S., Portela B.T.T., da Costa M., de Athaydes Silva Junior
652 J., … Meir P. (2010) Effect of 7 yr of experimental drought on vegetation dynamics and
653 biomass storage of an eastern Amazonian rainforest. *New Phytologist* **187**, 579–591.

654 da Costa A.C.L., Metcalfe D.B., Doughty C.E., de Oliveira A.A.R., Neto G.F.C., da Costa M.C., …
655 Malhi Y. (2014) Ecosystem respiration and net primary productivity after 8–10 years of
656 experimental through-fall reduction in an eastern Amazon forest. *Plant Ecology &*

Diversity **7**, 7–24.

Damián X., Fornoni J., Domínguez C.A. & Boege K. (2018) Ontogenetic changes in the phenotypic integration and modularity of leaf functional traits. *Functional Ecology*, 234–246.

Dayer S., Peña J.P., Gindro K., Torregrosa L., Voinesco F., Martínez L., … Zufferey V. (2017) Changes in leaf stomatal conductance , petiole hydraulics and vessel morphology in grapevine (Vitis vinifera cv . Chasselas) under different light and irrigation regimes. *Functional Plant Biology*, 679–693.

Dolan L. (2013) The New Phytologist Tansley Medal 2012. *New Phytologist* **197**, 1025–1026.

Domingues T.F., Meir P., Feldpausch T.R., Saiz G., Veenendaal E.M., Schrodt F., … Lloyd J. (2010) Co-limitation of photosynthetic capacity by nitrogen and phosphorus in West Africa woodlands. *Plant, Cell and Environment* **33**, 959–980.

Domingues T.F., MEIR P., Feldpausch T.R., Saiz G., Veenendaal E.M., Schrodt F., … Lloyd J. (2010) Co-limitation of photosynthetic capacity by nitrogen and phosphorus in West Africa woodlands. *Plant, Cell & Environment* **33**, 959–980.

Duffy P.B., Brando P., Asner G.P. & Field C.B. (2015) Projections of future meteorological drought and wet periods in the Amazon. *Proceedings of the National Academy of Sciences* **112**, 13172–13177.

Egea G., Gonzalez-Real M.M., Baille A., Nortes P.A., Conesa M.R. & Ruiz-Salleres I. (2012) Effects of water stress on irradiance acclimation of leaf traits in almond trees. *Tree Physiology* **32**, 450–463.

Eller C.B., Rowland L., Mencuccini M., Rosas T., Williams K., Harper A., … Cox P.M. (2020) Stomatal optimization based on xylem hydraulics (SOX) improves land surface model simulation of vegetation responses to climate. *New Phytologist* **226**, 1622–1637.

Eller C., de V. Barros F., R.L. Bittencourt P., Rowland L., Mencuccini M. & S. Oliveira R. (2018) Xylem hydraulic safety and construction costs determine tropical tree growth. *Plant, Cell & Environment* **41**, 548–562.

Fan L., Wigneron J.-P., Ciais P., Chave J., Brandt M., Fensholt R., … Peñuelas J. (2019) Satellite-observed pantropical carbon dynamics. *Nature Plants* **5**, 944–951.

Fu R., Yin L., Li W., Arias P.A., Dickinson R.E., Huang L., … Myneni R.B. (2013) Increased dry-season length over southern Amazonia in recent decades and its implication for future climate projection. *Proceedings of the National Academy of Sciences* **110**, 18110–18115.

Green J.K., Seneviratne S.I., Berg A.M., Findell K.L., Hagemann S., Lawrence D.M. & Gentine P. (2019) Large influence of soil moisture on long-term terrestrial carbon uptake. *Nature* **565**, 476–479.

Groenendijk P., Sass-Klaassen U., Bongers F. & Zuidema P.A. (2014) Potential of tree-ring analysis in a wet tropical forest: A case study on 22 commercial tree species in Central Africa. *Forest Ecology and Management* **323**, 65–78.

Houghton R.A. (2005) Aboveground Forest Biomass and the Global Carbon Balance. *Global Change Biology* **11**, 945–958.

Hubau W., Lewis S.L., Phillips O.L., Affum-Baffoe K., Beeckman H., Cuní-Sanchez A., … Zemagho L. (2020) Asynchronous carbon sink saturation in African and Amazonian tropical forests. *Nature* **579**, 80–87.

Hubau W., De Mil T., Van den Bulcke J., Phillips O.L., Angoboy Ilondea B., Van Acker J., … Beeckman H. (2019) The persistence of carbon in the African forest understory. *Nature Plants* **5**, 133–140.

Kamaluddin M. & Grace J. (1992) Acclimation in Seedlings of a Tropical Tree, Bischofia javanica, Following a Stepwise Reduction in Light. *Annals of Botany* **69**, 557–562.

705 Kramer P.J. (1988) Changing concepts regarding plant water relations. *Plant, Cell and*
706 *Environment* **11**, 565–568.

707 Krause G.H., Virgo A. & Winter K. (1995) High susceptibility to photoinhibition of young leaves
708 of tropical forest trees. *Planta* **197**, 583–591.

709 Li S., Lens F., Espino S., Karimi Z., Klepsch M., Schenk H.J., … Jansen S. (2016) Intervessel pit
710 membrane thickness as a key determinant of embolism resistance in angiosperm xylem.
711 *IAWA Journal* **37**, 152–171.

712 Love D.M. & Sperry J.S. (2018) In situ embolism induction reveals vessel refilling in a natural
713 aspen stand. *Tree Physiology* **38**, 1006–1015.

714 Lovejoy T.E. & Nobre C. (2019) Amazon tipping point: Last chance for action. *Science Advances*
715 **5**, 4–6.

716 Maherali H., Pockman W.T. & Jackson R.B. (2004) Adaptive variation in the vulnerability of
717 woody plants to xylem cavitation. *Ecology* **85**, 2184–2199.

718 Marengo J.A., Souza C.M., Thonicke K., Burton C., Halladay K., Betts R.A., … Soares W.R. (2018)
719 Changes in Climate and Land Use Over the Amazon Region: Current and Future Variability
720 and Trends. *Frontiers in Earth Science* **6**, 1–21.

721 Martin-StPaul N., Delzon S. & Cochard H. (2017) Plant resistance to drought depends on timely
722 stomatal closure. *Ecology Letters* **20**, 1437–1447.

723 Martin-StPaul N.K., Longepierre D., Huc R., Delzon S., Burlett R., Joffre R., … Cochard H. (2014)
724 How reliable are methods to assess xylem vulnerability to cavitation? The issue of “open
725 vessel” artifact in oaks. *Tree Physiology* **34**, 894–905.

726 Martinez-Vilalta J., Anderegg W.R.L., Sapes G. & Sala A. (2019) Greater focus on water pools
727 may improve our ability to understand and anticipate drought-induced mortality in

728 plants. *New Phytologist* **223**, 22–32.

729 Martínez-Vilalta J. & Garcia-Forner N. (2017) Water potential regulation, stomatal behaviour
730 and hydraulic transport under drought: deconstructing the iso/anisohydric concept. *Plant*
731 *Cell and Environment* **40**, 962–976.

732 McDowell N., Pockman W.T., Allen C.D., Breshears D.D., Cobb N., Kolb T., … Yepez E.A. (2008)
733 Mechanisms of plant survival and mortality during drought: why do some plants survive
734 while others succumb to drought? *New Phytologist* **178**, 719–739.

735 McDowell N.G., Beerling D.J., Breshears D.D., Fisher R.A., Raffa K.F. & Stitt M. (2011) The
736 interdependence of mechanisms underlying climate-driven vegetation mortality. *Trends*
737 *in Ecology and Evolution* **26**, 523–532.

738 Meinzer F.C., Johnson D.M., Lachenbruch B., McCulloh K.A. & Woodruff D.R. (2009) Xylem
739 hydraulic safety margins in woody plants: Coordination of stomatal control of xylem
740 tension with hydraulic capacitance. *Functional Ecology* **23**, 922–930.

741 Meir P., Mencuccini M. & Dewar R.C. (2015a) Drought-related tree mortality: addressing the
742 gaps in understanding and prediction. *New Phytologist* **207**, 28–33.

743 Meir P., Mencuccini M. & Dewar R.C. (2015b) Drought-related tree mortality: addressing the
744 gaps in understanding and prediction. *New Phytologist* **207**, 28–33.

745 Mencuccini M., Rosas T., Rowland L., Choat B., Cornelissen H., Jansen S., … Martínez–Vilalta J.
746 (2019) Leaf economics and plant hydraulics drive leaf : wood area ratios. *New Phytologist*
747 **224**, 1544–1556.

748 Metcalfe D.B., Meir P., Aragao L.E.O.C., Lobo-do-vale R., Galbraith D., Fisher R.A., … Gonc P.H.L.
749 (2010a) Shifts in plant respiration and carbon use efficiency at a large-scale drought
750 experiment in the eastern Amazon. *New Phytologist*, 608–621.

751 Metcalfe D.B., Meir P., Aragão L.E.O.C., Lobo-do-Vale R., Galbraith D., Fisher R.A., … Williams
752 M. (2010b) Shifts in plant respiration and carbon use efficiency at a large-scale drought
753 experiment in the eastern Amazon. *New Phytologist* **187**, 608–621.

754 Mulkey S.S. & Pearcy R.W. (1992) Interactions between Acclimation and Photoinhibition of
755 Photosynthesis of a Tropical Forest Understorey Herb, Alocasia macrorrhiza, during
756 Simulated Canopy Gap Formation. *Functional Ecology* **6**, 719.

757 Nardini A., Lo Gullo M.A. & Salleo S. (2011) Refilling embolized xylem conduits: Is it a matter of
758 phloem unloading? *Plant Science* **180**, 604–611.

759 Oliveira R.S., Costa F.R.C., Baalen E. Van, Jonge A. De, Bittencourt P.R., Almanza Y., … Poorter L.
760 (2019) Embolism resistance drives the distribution of Amazonian rainforest tree species along
761 hydro-topographic gradients. *New Phytologist*, 1457–1465.

762 Oren R. & Pataki D.E. (2001) Transpiration in response to variation in microclimate and soil
763 moisture in southeastern deciduous forests. *Oecologia* **127**, 549–559.

764 Pammenter N.W. & Van der Willigen C. (1998) A mathematical and statistical analysis of the
765 curves illustrating vulnerability of xylem to cavitation. *Tree Physiology* **18**, 589–593.

766 Pan Y., Birdsey R.A., Fang J., Houghton R., Kauppi P.E., Kurz W.A., … Hayes D. (2011) A Large
767 and Persistent Carbon Sink in the World's Forests. *Science* **333**, 988–993.

768 Pereira L., Bittencourt P.R.L., Oliveira R.S., Junior M.B.M., Barros F. V, Ribeiro R. V & Mazzafera
769 P. (2016) Plant pneumatics: stem air flow is related to embolism – new perspectives on
770 methods in plant hydraulics. *New Phytologist* **211**, 357–370.

771 Pereira L. & Mazzafera P. (2013) A low cost apparatus for measuring the xylem hydraulic
772 conductance in plants. *Bragantia* **71**, 583–587.

773 Poorter H., Niinemets Ü., Poorter L., Wright I.J. & Villar R. (2009) Causes and consequences of

774 variation in leaf mass per area (LMA): a meta−analysis. *New Phytologist* **182**, 565–588.

775 Powell T.L., Wheeler J.K., de Oliveira A.A.R., da Costa A.C.L., Saleska S.R., Meir P. & Moorcroft
776 P.R. (2017) Differences in xylem and leaf hydraulic traits explain differences in drought
777 tolerance among mature Amazon rainforest trees. *Global Change Biology* **23**, 4280–4293.

778 Prendin A.L., Mayr S., Beikircher B., von Arx G. & Petit G. (2018) Xylem anatomical adjustments
779 prioritize hydraulic efficiency over safety as Norway spruce trees grow taller. *Tree*
780 *Physiology* **38**, 1088–1097.

781 Rowland L., da Costa A.C.L., Galbraith D.R., Oliveira R.S., Binks O.J., Oliveira A.A.R., … Meir P.
782 (2015a) Death from drought in tropical forests is triggered by hydraulics not carbon
783 starvation. *Nature* **528**, 119–122.

784 Rowland L., Lobo-do-Vale R.L., Christoffersen B.O., Melém E.A., Kruijt B., Vasconcelos S.S., …
785 Meir P. (2015b) After more than a decade of soil moisture deficit, tropical rainforest trees
786 maintain photosynthetic capacity, despite increased leaf respiration. *Global Change*
787 *Biology* **21**, 4662–4672.

788 Rowland L., da Costa A.C.L., Oliveira R.S., Bittencourt P.R.L., Giles A.L., Coughlin I., … Meir P.
789 (2020) The response of carbon assimilation and storage to long−term drought in tropical
790 trees is dependent on light availability. *Functional Ecology*, 1365-2435.13689.

791 Ruggiero P.G.C., Batalha M.A., Pivello V.R. & Meirelles S.T. (2002) Soil vegetation relationships
792 in cerrado (Brazilian savanna) and semideciduous forest, Southeastern Brazil. *Plant*
793 *Ecology* **160**, 1–16.

794 Salleo S., Lo Gullo M.A., De Paoli D. & Zippo M. (1996) Xylem recovery from cavitation-induced
795 embolism in young plants of Laurus nobilis: A possible mechanism. *New Phytologist* **132**,
796 47–56.

797 Salleo S., Lo Gullo M.A., Trifilò P. & Nardini A. (2004) New evidence for a role of vessel-

798 associated cells and phloem in the rapid xylem refilling of cavitated stems of Laurus
799 nobilis L. *Plant, Cell and Environment* **27**, 1065–1076.

800 Schneider C.A., Rasband W.S. & Eliceiri K.W. (2012) NIH Image to ImageJ: 25 years of image
801 analysis. *Nature Methods* **9**, 671–675.

802 Schuldt B., Leuschner C., Horna V., Moser G., Köhler M., Van Straaten O. & Barus H. (2011)
803 Change in hydraulic properties and leaf traits in a tall rainforest tree species subjected to
804 long-term throughfall exclusion in the perhumid tropics. *Biogeosciences* **8**, 2179–2194.

805 Sperry J.S., Hacke U.G., Oren R. & Comstock J.P. (2002) Water deficits and hydraulic limits to
806 leaf water supply. *Plant, Cell and Environment*, 251–263.

807 Sperry J.S. & Tyree M.T. (1988) Mechanism of Water Stress-Induced Xylem Embolism1. *Plant*
808 *physiology* **88**, 581–587.

809 Sperry J.S., Venturas M.D., Anderegg W.R.L., Mencuccini M., Mackay D.S., Wang Y. & Love D.M.
810 (2017a) Predicting stomatal responses to the environment from the optimization of
811 photosynthetic gain and hydraulic cost. *Plant Cell and Environment* **40**, 816–830.

812 Sperry J.S., Venturas M.D., Anderegg W.R.L., Mencuccini M., Mackay D.S., Wang Y. & Love D.M.
813 (2017b) Predicting stomatal responses to the environment from the optimization of
814 photosynthetic gain and hydraulic cost. *Plant, Cell & Environment* **40**, 816–830.

815 Sterck F., Anten N.P.R., Schieving F. & Zuidema P.A. (2016a) Trait Acclimation Mitigates
816 Mortality Risks of Tropical Canopy Trees under Global Warming. *Frontiers in Plant Science*
817 **7**, 1–10.

818 Sterck F., Anten N.P.R., Schieving F. & Zuidema P.A. (2016b) Trait Acclimation Mitigates
819 Mortality Risks of Tropical Canopy Trees under Global Warming. *Frontiers in Plant Science*
820 **7**.

821 Tardieu F. (1996) Drought perception by plants: Do cells of draughted plants experience water
822 stress? *Plant Growth Regulation* **20**, 93–104.

823 Tng D.Y.P., Apgaua D.M.G., Ishida Y.F., Mencuccini M., Lloyd J., Laurance W.F. & Laurance
824 S.G.W. (2018) Rainforest trees respond to drought by modifying their hydraulic
825 architecture. *Ecology and Evolution* **8**, 12479–12491.

826 Tomasella M., Beikircher B., Häberle K.H., Hesse B., Kallenbach C., Matyssek R. & Mayr S.
827 (2018) Acclimation of branch and leaf hydraulics in adult Fagus sylvatica and Picea abies
828 in a forest through-fall exclusion experiment. *Tree Physiology* **38**, 198–211.

829 Trugman A.T., Detto M., Bartlett M.K., Medvigy D., Anderegg W.R.L., Schwalm C., … Pacala S.W.
830 (2018) Tree carbon allocation explains forest drought-kill and recovery patterns. *Ecology*
831 *Letters*, 1552–1560.

832 Venturas M.D., Mackinnon E.D., Jacobsen A.L. & Pratt R.B. (2015) Excising stem samples
833 underwater at native tension does not induce xylem cavitation. *Plant, Cell and*
834 *Environment* **38**, 1060–1068.

835 Wright I.J., Reich P.B., Westoby M., Ackerly D.D., Baruch Z., Bongers F., … Gulias J. (2004) The
836 worldwide leaf economics spectrum. *Nature* **12**, 821–827.

837 Yang Y., Saatchi S.S., Xu L., Yu Y., Choi S., Phillips N., … Myneni R.B. (2018) Post-drought decline
838 of the Amazon carbon sink. *Nature Communications* **9**, 3172.

839 Yuan W., Zheng Y., Piao S., Ciais P. & Lombardozzi D. (2019) Increased atmospheric vapor
840 pressure deficit reduces global vegetation growth. *Science Advances*, 1–14.

841 Yue X., Zuo X., Yu Q., Xu C., Lv P., Zhang J., … Smith M.D. (2019) Response of plant functional
842 traits of Leymus chinensis to extreme drought in Inner Mongolia grasslands. *Plant*
843 *Ecology* **220**, 141–149.

Zhang Y., Lamarque L.J., Torres-Ruiz J.M., Schuldt B., Karimi Z., Li S., … Jansen S. (2018) Testing the plant pneumatic method to estimate xylem embolism resistance in stems of temperate trees. *Tree Physiology* **38**, 1016–1025.

Table 1 – Mean and standard deviation of P_{50} - xylem embolism resistance (MPa); P_{88} - xylem embolism resistance (MPa); Ψ_{pd} - predawn water potential (MPa); Ψ_{md} - midday water potential (MPa); HSM – hydraulic safety margin to P_{50} (MPa); PLC – native dry season percentage loss of conductivity (%); K_s – maximum hydraulic specific conductivity (kg m^{-2} s^{-1} MPa^{-1}); W_D- Woody density; K_{sl} - maximum hydraulic leaf-specific conductivity (kg m^{-2} s^{-1} MPa^{-1}); A_L:A_{SW} – leaf to sapwood area ratio (m^2 m^{-2}); G_{min} – minimum stomatal conductance (mol m^{-2} s^{-1}), separated by genus and treatment.

		Hydraulics traits										
Genus	**Treatment**	**P_{50}**	**P_{88}**	**G_{min}**	**K_s**	**K_{sl}**	**A_L:A_{SW}**	**W_D**	**Ψ_{pd}**	**Ψ_{md}**	**HSM**	**PLC**
Eschweilera	**Control**	-2.91±0.07	-5.08±0.31	0.028±0.023	1.12±0.19	0.57±0.30	112.07±32.41	0.73±0.12	-0.32±0.23	-1.68±0.24	1.13±0.32	49.14±4.9
Eschweilera	**TFE**	-3.66±2.01	-6.32±3.80	0.026±0.019	2.80±2.62	4.71±6.12	92.12±65.44	0.59±0.09	-0.52±0.24	-1.87±0.26	1.89±2.28	9.22±4.36
Inga	**Control**	-4.60±1.63	-7.84±3.10	0.02±0.014	2.3±1.43	1.56±0.85	84.59±47.51	0.64±0.18	-0.37±0.26	-1.51±0.57	3.09±2.07	11.33±10.19
Inga	**TFE**	-3.48±0.58	-6.22±1.62	0.02±0.006	4.56±1.68	1.93±0.73	160.81±58.68	0.63±0.08	-0.39±0.22	-1.35±0.78	2.13±0.4	19.28±13.21
Licania	**Control**	-5.28±1.98	-9.62±4.40	0.025±0.014	0.15±0.04	0.12±0.072	66.15±24.41	0.76±0.062	-0.25±0.07	-1.65±0.85	3.62±2.75	38.29±28.52
Licania	**TFE**	-6.18±1.59	-9.07±1.77	0.024±0.02	2.17±2.19	0.37±0.40	104.90±45.99	0.761±0.014	-0.85±0.81	-1.388±0.789	5.183±1.701	68.667±28.13
Mouriri	**Control**	-4.77±0.54	-7.69±1.31	0.025±0.017	0.62±0.051	0.22±0.20	154.33±59.51	0.867±0.003	-0.24±0.09	-0.943±0.081	3.829±0.48	58.031±27.65
Mouriri	**TFE**	-5.55±0.74	-7.35±2.18	0.077±0.022	3.63±3.036	1.32±0.88	143.30±92.13	0.751±0.176	-1.07±1.32	-2.583±0.957	2.972±0.776	60.769±15.83
Ocotea	**Control**	-3.59±1.49	-8.72±2.63	0.007±0.003	1.63±0.81	0.84±0.17	125.38±54.22	0.638±0.054	-0.36±0.4	-0.6±0.364	2.994±1.267	36.718±18.42
Ocotea	**TFE**	-5.04±2.08	-8.61±4.88	0.03±0.024	1.58±0.66	0.60±0.46	84.83±32.64	0.68±0.13	-1.44±1.17	-2.41±0.81	2.62±2.45	65.27±24.19
Protium	**Control**	-2.30±0.71	-4.16±2.40	0.017±0.012	1.68±0.94	0.75±0.41	78.60±6.37	0.74±0.07	-0.332±0.3	-1.23±0.314	1.07±0.78	54.73±17.02
Protium	**TFE**	-3.64±1.47	-5.65±0.73	0.013±0.011	1.10±0.07	0.44±0.07	90.57±17.71	0.72±0.049	-0.48±0.16	-1.00±0.24	2.55±1.73	49.74±11.94
Swartzia	**Control**	-3.17±1.28	-5.98±1.89	0.06±0.042	1.67±0.26	0.78±0.55	72.45±18.20	0.73±0.02	-0.23±0.12	-1.57±0.161	1.60±1.36	59.73±9.94
Swartzia	**TFE**	-4.34±0.57	-6.94±0.06	0.06±0.02	2.78±0.51	0.89±0.54	210.45±67.51	0.72±0.005	-0.79±0.48	-2.36±0.09	1.98±0.66	49.13±8.57
Tetragastris	**Control**	-2.31±1.48	-4.34±1.81	0.03±0.01	2.22±1.66	2.29±3.12	83.86±59.38	0.64±0.05	-0.28±0.13	-1.06±0.58	1.25±1.31	22.12±15.60
Tetragastris	**TFE**	-4.36±1.19	-6.52±2.90	0.016±0.011	1.33±0.62	1.04±0.45	88.10±34.28	0.58±0.04	-1.43±0.4	-2.44±0.139	1.92±1.06	43.24±6.33
Vouacapoa	**Control**	-3.57±0.13	-5.37±1.45	0.015±0.003	1.00±0.16	0.95±0.64	56.71±22.69	0.69±0.13	-0.39±0.18	-1.59±0.19	1.97±0.31	43.78±11.37
Vouacapoa	**TFE**	-2.22±0.79	-3.54±1.63	0.012±0.004	0.83±0.51	0.67±0.78	229.76±101.26	0.70±0.01	-0.77±0.35	-2.07±0.24	0.15±0.72	33.24±19.67

858

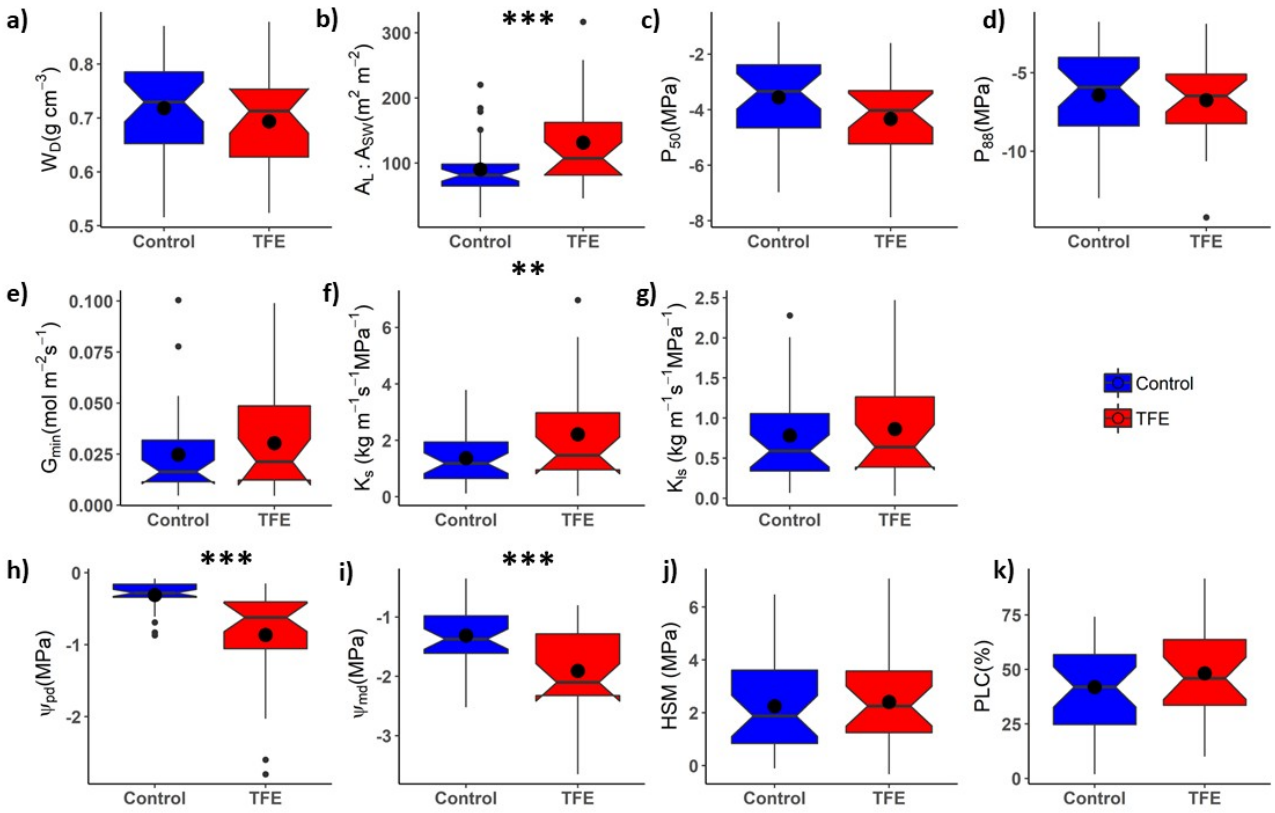

Figure 1 Stress indicators and hydraulic traits on the control plot (blue) and through-fall exclusion (TFE, red). a) W_D – wood density b) A_L:A_{SW} - leaf to sapwood area ratio c) P_{50} - xylem embolism resistance; d) P_{88} - xylem embolism resistance; e) G_{min} – minimum stomatal conductance; f) K_s – maximum hydraulic specific conductivity; g) K_{sl} - maximum hydraulic leaf - specific conductivity; h) Ψ_{pd} - predawn water potential; i)Ψ_{md} - midday water potential. j) HSM – hydraulic safety margin to P_{50}; l) PLC – native dry season percentage loss of conductivity. The boxes represent quartiles 1 and 3, with the central line indicating the median. The central points represent the mean by each treatment. Whiskers are either maximum value or 1.5 interquartile range above quartile 3, if outliers are present and notches represents a confidence interval around the median represented by central line. Traits for which plot had a significant effect are marked with * ($p < 0.05$), ** ($p < 0.01$) and *** ($p < 0.001$). P-values are from mixed effects analysis (see Table 2 for models and analysis section in Methods

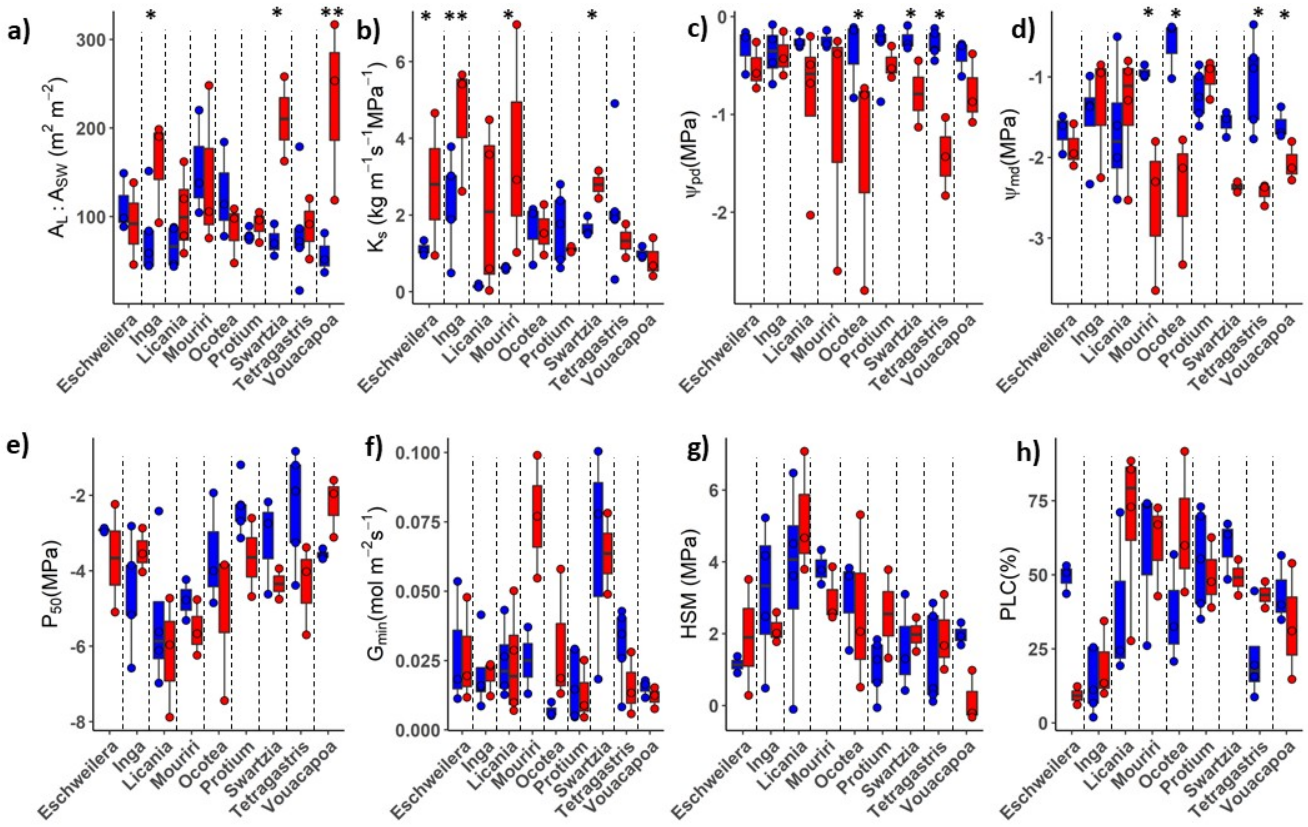

873 **Figure 2** Drought stress indicators and hydraulic traits considered by genus on trees surviving
874 after 15 years of throughfall exclusion (TFE – red) and the control plot (blue). a) A_L:A_{SW} - leaf to
875 sapwood area ratio (m^2 m^{-2}); b) K_s – maximum hydraulic specific conductivity; c) Ψ_{pd} - predawn
876 water potential; d) Ψ_{md} - midday water potential; e) P_{50} - xylem embolism resistance; f) G_{min} –
877 minimum stomatal conductance g) HSM– hydraulic safety margin to P_{50}; h) PLC – native dry
878 season percentage loss of conductivity. The box represents quartiles 1 and 3, with the central
879 line indicating the median. Whiskers are either maximum value or 1.5 interquartile range
880 above the quartile 3, when outliers are present. The points represent individuals by species in
881 each treatment. Traits for which plot had a significant effect are marked with * ($p < 0.05$), ** (p
882 < 0.01) and *** ($p < 0.001$). P-values are from mixed effects analysis (see Table 2 for models
883 and analysis section in Methods.

884

885

Table 2. Results of linear mixed effect models of plot (Control versus TFE) on the four key hydraulic variables (A_L: A_{SW}- Leaf to sapwood area ratio; K_s – maximum hydraulic specific conductivity; Ψ_{pd} - predawn water potential; Ψ_{md} - midday water potential, all of which showed significant changes between the TFE and Control plots. Intercept is the Control and the Plot effect is the difference of the TFE from the Control and random genus effects (on intercept is control effect and Plot effect) are shown (see analysis section in Methods for details). The Numbers under Random Effects is standard deviation and under Fixed effects is coefficient values ± standard error. Significant intercept and fixed effects parameters are shown from F test with a standard error. Marginal (fixed effects only) and conditional R^2 (random and fixed effects) are shown (Mulkey & Pearcy 1992). The effect of species nested within genus was tested and with the exception of Ks, it did not yield a model with lower AIC than genus alone (Table S3).

	Fixed Effects		**Random Effects**				
Variable	**Intercept**	**Plot**	**Intercept**	**Plot**	**Residual**	**R^2 M**	**R^2 C**
K_s	1.37±0.28***	1.02±0.43*	0.59	-	1.37	0.11	0.25
A_L:A_{SW}	87.65 ± 11.18**	54.68±17.09**	-	-	-	0.17	0.17
Ψ_{pd}	-0.31 ± 0.09**	-0.43± 0.14***	-	-	-	0.16	0.16
Ψ_{md}	-1.78 ± 0.13***	-0.60 ± 0.27 *	0.26	0.71	0.52	0.12	0.44

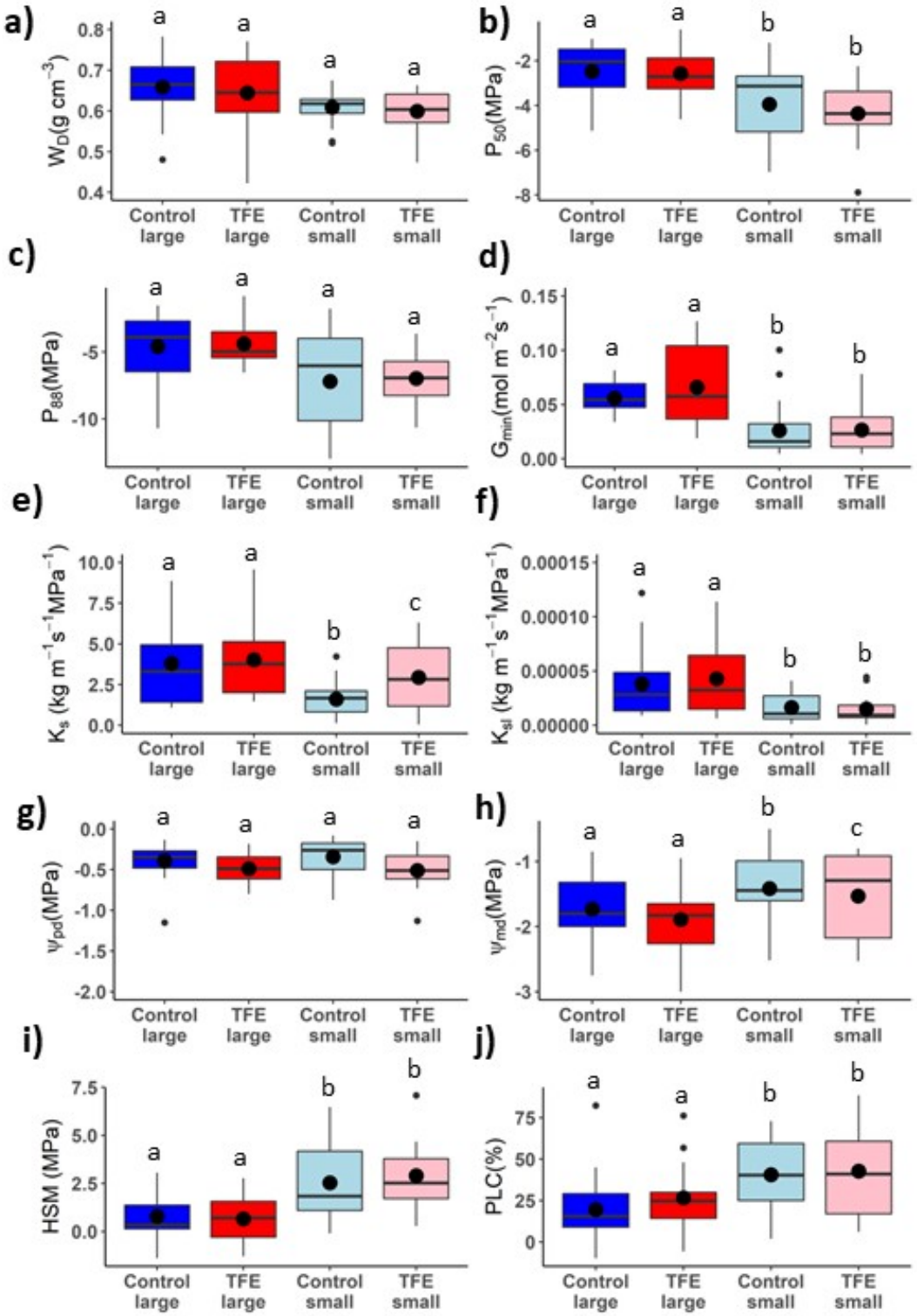

Figure 3 Comparison between small trees and adult tress from the throughfall exclusion (TFE) and Control plots. a) W_D – wood density; b) P_{50} - xylem embolism resistance; c) P_{88} - xylem embolism resistance; d) G_{min} – minimum stomatal conductance; e) K_s – maximum hydraulic specific conductivity; f) K_{sl} - maximum hydraulic leaf -specific conductivity; g) Ψ_{pd} - predawn

905 water potential; h) Ψ_{md} midday water potential; i) PLC – native dry season percentage loss of
906 conductivity; j) HSM – hydraulic safety margin to P_{50}. The box represents quartiles 1 and 3, with
907 the central line indicating the median. Whiskers are either maximum value or 1.5 interquartile
908 range above the quartile 3, when outliers are present. Different letter indicant significant
909 differences, $p<0.001$.

910

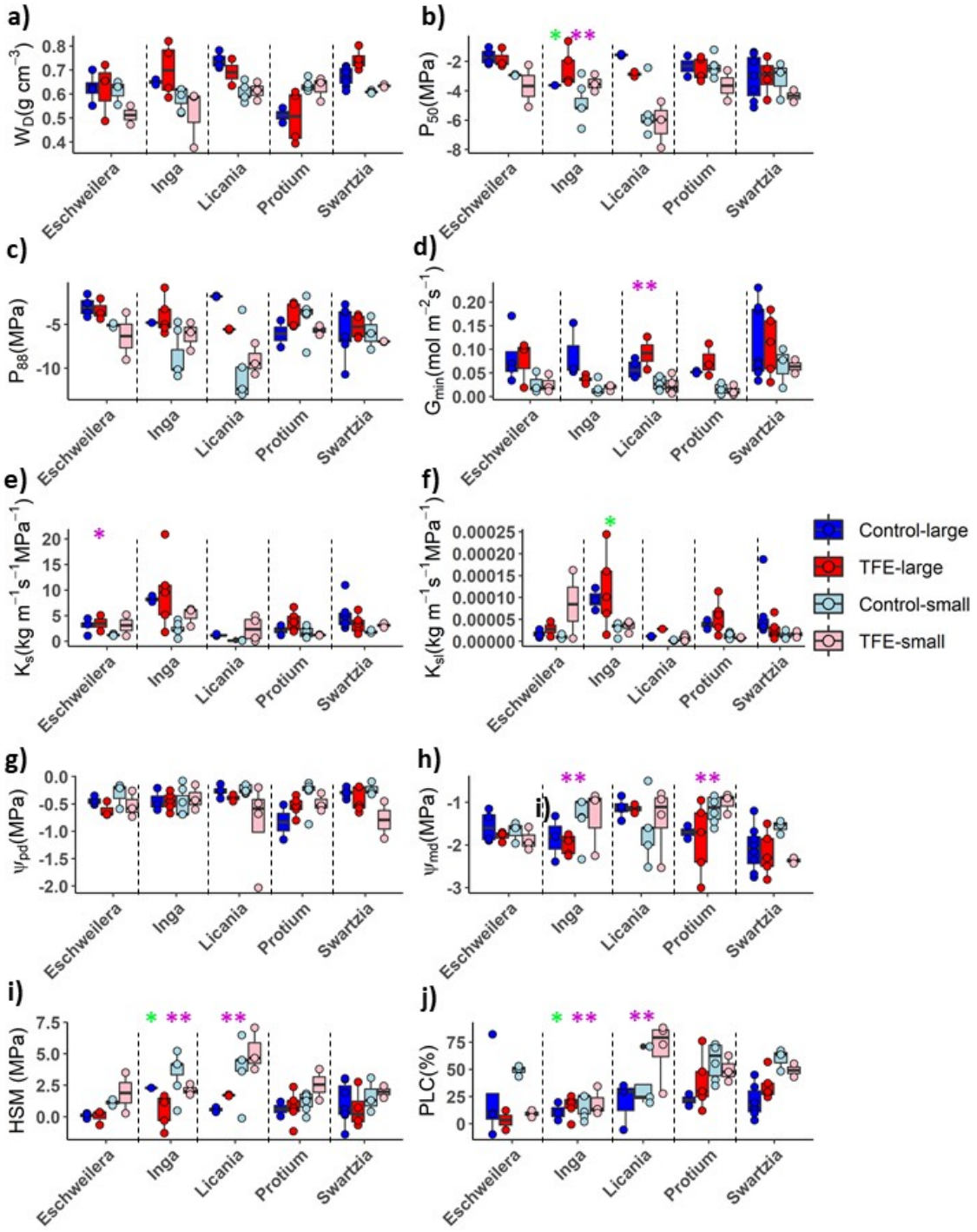

Figure 4 Comparison between small trees and adult trees from throughfall exclusion (TFE) and control plot. a) W_D – wood density ; b) P_{50} - xylem embolism resistance; c) P_{88} - xylem embolism resistance; d) G_{min} – minimum stomatal conductance; e) K_s – maximum hydraulic specific conductivity; f) K_{sl} - maximum hydraulic leaf -specific conductivity; g) Ψ_{pd} - predawn water potential ; h) Ψ_{md} midday water potential; i) HSM – hydraulic safety margin to P_{50}; j) PLC –

native dry season percentage loss of conductivity. The box represents quartiles 1 and 3, with the central line indicating the median. Whiskers are either maximum value or 1.5 interquartile range above the quartile 3, when outliers are present. Traits for which plot had a significant effect are marked with a green asterisk and traits for which size had a significant effect are marked with pink asterisk. P-values are from Wilcox test * ($p < 0.05$), ** ($p < 0.01$) and *** ($p < 0.001$).

Table 3. Results of linear mixed effect models of size (large trees versus small understorey trees) and plot effect (TFE and Control) on drought stress indicators and hydraulic traits. We tested the random genus effects on intercept and/or on plot and size (see Methods). Values for fixed effects are fitted parameter ± standard error. Values for Intercept column indicate the mean of the variable of large trees in Control plot, and the size column indicates of values of small trees on average in relation to large trees. Values for plot column indicate the values on the TFE plot in relation to control plot. Values of size:plot column indicates the mean values of the interaction of small trees on TFE plot in relation Control and Large trees. Values for random effects are the standard deviation of the normal distribution from which coefficients were fitted. Marginal (R^2m - fixed effects only) and conditional R^2 (R^2c -random and fixed effects) are shown (Nakagawa & Schielzeth, 2013). Blank cells indicate that the effect is non-significant. P_{50} - xylem embolism resistance (MPa); G_{min} – minimum stomatal conductance (mol m^{-2} s^{-1}); K_s – maximum hydraulic specific conductivity (kg m^{-1} s^{-1} MPa^{-1}); Ψ_{md} - midday water potential (MPa); HSM – hydraulic safety margin to P_{50} (MPa); PLC – native dry season percentage loss of conductivity (%); * p < 0.05; ** p < 0.01; *** p < 0.001.

Variables	**Fixed effect**				**Random effect**			**R^2m**	**R^2c**
	Intercept	**Size (small)**	**Plot (TFE)**	**Size:plot**	**Intercept**	**Plot**	**Resid.**		
P_{50}	-2.64 ± 0.16***	-1.33±0.51**			0.98		1.12	0.20	0.39
G_{smin}	-0.08±0.007*	-0.05±0.008			0.013		0.04	0.23	0.30
K_s	4.05±1.03**	-2.58±0.90*	0.45±0.6**	1.08±1.00	2.05	1.36	2.29	0.14	0.44
K_{ls}	6.13±0.45	-1.13 ±0.42			0.85		2.01	0.11	0.33
Ψ_{md}	-1.75 ± 0.12***	-0.60 ± 0.27 *			0.24		0.48	0.04	0.24
HSM	0.89± 0.30**	1.70± 0.31***			0.49		1.37	0.25	0.33
PLC	19.80± 4.74***	22.20±4.07			8.92		19.13	0.20	0.34